

ABSTRACT

Modelling the vulnerability of houses in windstorms is important for insurance pricing, policy-making, and emergency management. Vulnerability models for Australian house types have been developed since the 1970s and have ranged from empirical models to more advanced reliability based structural engineering models, which provide estimates of damage for a range of wind speeds of interest. This paper describes recent developments in the engineering based vulnerability modelling software: 'Vulnerability and Adaption to Wind Simulation' (VAWS), which uses probability based reliability analysis and structural engineering for the loading and response coupled with an extensive test database and field damage assessments to calculate the damage experienced by selected Australian house types. A case study is presented to demonstrate the program's ability to model progressive failures, internal pressurization and debris impact.

Modelling the vulnerability of a high-set house roof structure to windstorms using VAWS

■ Korah Parackal^{1,3}, Martin Wehner^{2,3}, Hyeuk Ryu^{2,3}, John Ginger^{1,3}, Daniel Smith^{1,3}, David Henderson^{1,3} and Mark Edwards^{2,3}

1. Cyclone Testing Station, James Cook University.
2. Geoscience Australia.
3. Bushfire and Natural Hazards CRC.

Vulnerability and Adaptation to Wind Simulation (VAWS) is a software package that can be used to model the vulnerability of small buildings such as domestic houses and light industrial sheds to wind (Geoscience Australia, 2019, Wehner et al., 2010a). The primary aim of VAWS is the estimation of the change in vulnerability afforded by mitigation measures to improve a building's resilience to wind storms.

VAWS consists of probabilistic modules for the 1. Wind hazard – external and internal pressures generated by the atmospheric wind and 2. Structural response – related to the structural system and capacities of the components and connections and load effects. The program is able to accommodate a range of house types for which the structural system, connections and the external pressure distribution for wind exposure from directions around the compass is applied as input data.

The critical structural components are probabilistically assigned their strengths and the wind loads are applied for winds approaching from a selected direction. Failure is initiated when the load exceeds the capacity of a critical component or connection as the wind loads are increased with increasing discrete wind speed increments. When components fail, loads are redistributed through the structural system. The cost of repair is calculated for the given level of damage and the damage index is calculated at each wind speed increment.

This paper describes the logic of VAWS including the main modules: the house type and structural system, external and internal pressure distribution, structural response, initiation and progression of damage, windborne debris impact, water ingress and cost of repair. A case study is presented to show the preliminary outputs of VAWS for a high-set Northern Australian house type.

Overall logic

The program is built around the high level sequence flow chart shown in Figure 1. The VAWS program takes a component-based approach to modelling building vulnerability. It is based on the premise that overall building damage is strongly related to the failure of key structural connections. The program generates a building model by selecting parameter values from predetermined probability distributions using a Monte Carlo process. Values include component and connection strengths, external pressure coefficients, shielding coefficients, wind speed profile with height, building orientation,

debris damage parameters, and component masses. Then, for increasing gust wind speed increments, it calculates the forces in all critical connections using influence coefficients, assesses which connections have failed and translates these into a damage scenario and costs the repair. Using the repair cost and the full replacement cost, it calculates a damage index at each wind speed.

Key Parameters and Variability

The Monte Carlo process captures a range of variability in both wind loading and component parameters. The parameter values are sampled for each realisation of the modelled house and kept the same as the wind speed is incremented up to a set maximum.

- Wind direction: For each house, its orientation with respect to the approach wind is chosen from the eight cardinal directions either randomly, or set constant by the user.
- Gust wind profile: Variation in the profile of wind speed with height is captured by the random sampling of a profile from a suite of user-provided profiles related to the approach terrain.
- External pressure coefficients for zones and coverages: External pressure coefficients for different zones of the house surfaces envelope are randomly

chosen from a Type III (Weibull) extreme value distribution based on wind tunnel data, with specified means and coefficients of variation for different zones of the house envelope.

- Strength and dead load: Connection strengths and dead loads for each realization are sampled from lognormal probability distributions specified by the user.

Water ingress: is estimated in order to account for the large costs associated with water damage to internal linings. Predefined relationships for water damage as a function of wind speed are selected based on the extent of damage to the house envelope.

Structural Response and Load Redistribution

The VAWS program accounts for load redistribution and progressive failures of the roof structure without the use of computationally intensive non-linear structural analysis by incorporating several simplifying assumptions. Connections considered in the analysis include: cladding fasteners, batten to rafter connections and rafter to top plate connections.

The program relates pressures applied to envelope zones to the cladding connection loads and the supporting structure using linear elastic influence coefficients. Once connections have failed, the effects of redistribution are preserved for

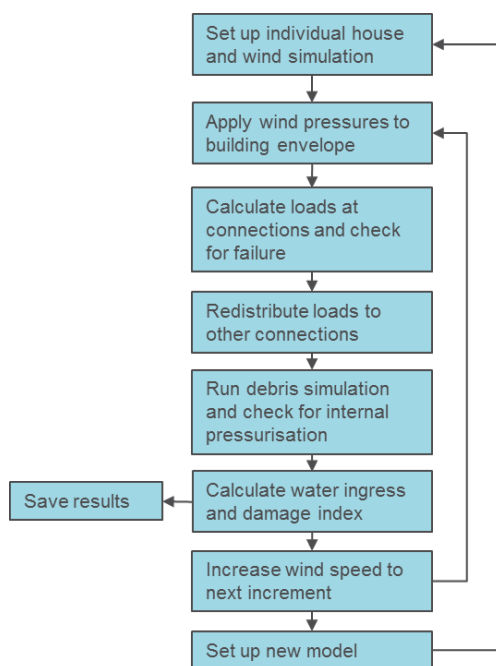


Figure 1: Vulnerability and Adaption to Wind Simulation (VAWS) program logic.

successive wind speed increments, thus ensuring that increasing wind loads act on the damaged structure rather than beginning anew with an intact structure. Following connection failures, redistribution of loads is modelled by changing the values of influence coefficients depending on the position of the failed connection in the load path.

Damage Costing

The program determines a repair cost for a damaged house by modelling the damage state(s) which a house is in at each wind speed and then costing the required repair work. The modelled house may have experienced one or more damage states (for example, loss of roof sheeting and debris damage to walls). The repair cost for any particular damage state is made up of two components: repair to damage to the external envelope and repair of consequential damage to the interior with repair of interior damage caused by water ingress calculated separately. Thus, the total repair cost for a house type at a wind speed is expressed as:

$$\begin{aligned} &\text{Total repair cost} \\ &= \left(\sum_{\text{All damage states } i} \text{External envelope repair cost}_i \right. \\ &\quad \left. + \text{Consequential internal repair cost}_i \right) \\ &\quad + \text{Water ingress repair cost} \end{aligned}$$

The two components of the repair cost for each damage state i are calculated as below. The calculation allows for each damage state to only affect part of the total susceptible area (for example, only a corner of the roof may have lost its roof sheeting).

$$\begin{aligned} \text{External envelope repair cost}_i &= \text{Total quantity}_i \times \text{Percent damage}_i \\ &\quad \times \text{Repair rate}_i \times f_i(\text{Percent damage}) \end{aligned}$$

$$\begin{aligned} \text{Consequential internal repair cost}_i &= \text{Internal repair cost}_i \times \text{Percent damage}_i \\ &\quad \times f_i(\text{Percent damage}) \end{aligned}$$

Where $f_i(\text{Percent damage})$ are functions adjusting the repair rate to allow for higher repair rates for extents of repair less than full repair. It is in the form of a quadratic equation ($a_1x^2 + a_2x + a_3$) where x is the percent damage in a particular damage state and a_1 to a_3 are supplied coefficients.

The repair cost due to water ingress is calculated from the modelled degree of water ingress, the dominant damage state and repair costs supplied in the costing data as follows.

$$\begin{aligned} \text{Water ingress repair cost}_i &= \text{Water ingress repair cost}_{i,\%} \\ &\quad \times f_i(\text{Percent damage}) \end{aligned}$$

Where Water ingress repair cost $_{i,\%}$ is repair cost data supplied as part of the costing module for repair of damage caused by water ingress for a house. The costing algorithm contains logic to prevent double counting of repair to building components where component repair is nominated in multiple damage states.

The project expresses repair costs as a damage index calculated as:

$$\text{Damage Index} = \frac{\text{Total building repair cost}}{\text{Building replacement cost}}$$

This permits the results to be applied to other houses of similar generic type but different floor areas. The repair cost is then calculated by multiplying the damage index by the floor area and the replacement rate for the generic house type.

Case study: vulnerability of a high-set northern Australian house

The Group 4 house

The VAWS software was used to model the vulnerability of the roof of a high-set Northern Australian house. The model details and an interpretation of the results are presented in the following sections. The house is a high-set timber framed structure with metal roof cladding and fiber cement wall cladding, an example shown in Figure 2. The dimensions and structural system were determined from survey data and the resulting representative house was originally described in Henderson and Harper (2003) as the Group 4 House. Further study on the vulnerability of this house types was performed by Henderson and Ginger (2007).

The house is 12.6 m long, 7.3 m wide and 4.4 m tall including 2.0 m stumps. The roof structure consists of rafters at 10° pitch spaced at nominally 900 mm centers supporting battens also at 900 mm centers, which support corrugated metal cladding. The overall dimensions and locations of windows and doors are shown in

Figure 3. A schematic of the roof structure and a framing plan showing the locations of battens and rafters is shown in Figure 4.

Assumptions

This case study focuses on the modelling of structural damage to the roof of a population of Group 4 Houses. In order for the damage index to represent the cost of repair of structural damage, certain settings are implemented to ensure the extent of damage is calculated based on structural damage alone:

- Damage induced by water ingress is ignored.
- Debris damage is not costed so that the damage index excludes the cost of repair of wall cladding but allows for the effects of internal pressures.



Figure 2: Example of a Group 4 House type Henderson and Ginger (2007).

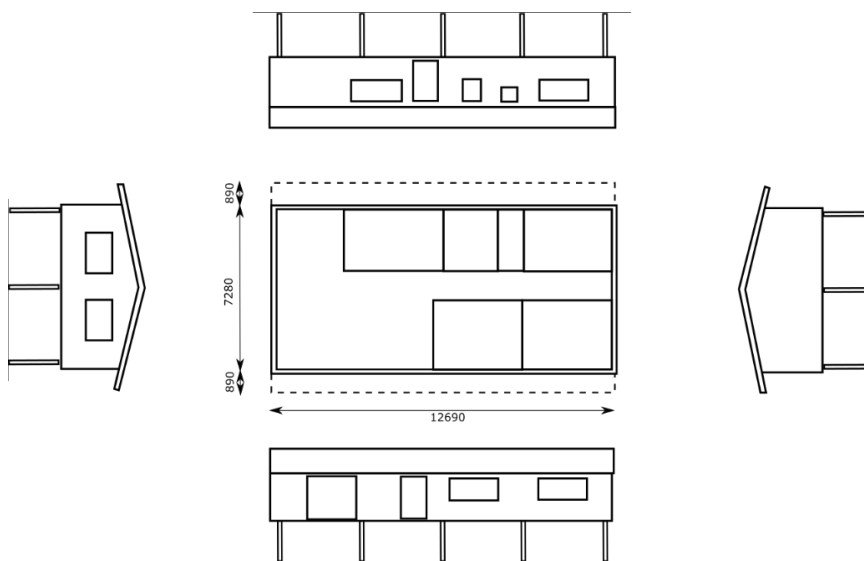


Figure 3: Overall dimensions of the Group 4 House, dimensions in mm.

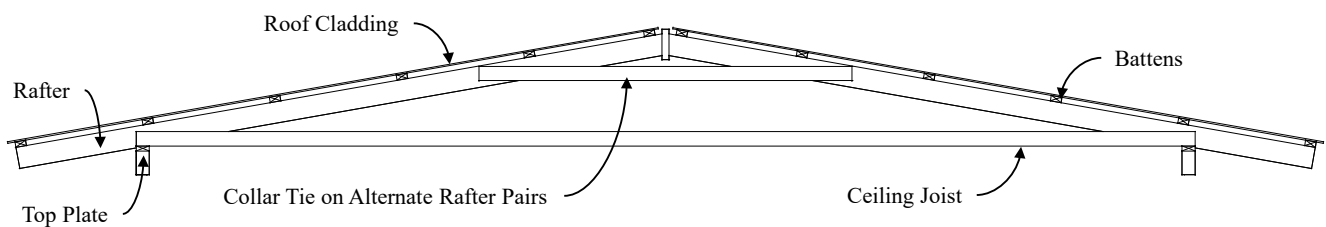


Figure 4: Roof structure of the Group 4 House.

Inputs

Wind pressures

Wind loads on the Group 4 House were determined by carrying out a wind tunnel model study. The model used was originally tested by Holmes and Best (1978) and has similar dimensions to the Group 4 House. The model was modified to reduce the size of the eaves to be more representative of the Group 4 House.

The tests were carried out in the 2.0 m high × 2.5 m wide × 22 m long boundary layer wind tunnel at the Cyclone Testing Station, James Cook University. The approach atmospheric boundary layer profile (suburban terrain, category 2.5 as per AS/NZS 1170.2) was simulated at a length scale of 1/50 using a 250 mm high trip board at the upstream end followed by an array of blocks on the tunnel floor.

Pressure taps were installed on the roof, wall and the floor of the model to measure the external pressures. Each pressure tap was connected to transducers located below the wind tunnel floor/turntable via a length of tuned PVC tubing. External pressures on the roof, walls and floor were obtained for approach wind directions (θ) of 0° to 360° in steps of 10°. The fluctuating pressures were low-pass filtered at 500 Hz, sampled at 1000 Hz for 30 s (corresponding to ~ 10 min in full-scale) and recorded as $p(t)$ and statistically analyzed to give mean, maximum and minimum pressure coefficients referenced to the mean dynamic pressure at roof height:

$$C_{\bar{p}} = \frac{\bar{p}}{\frac{1}{2}\rho\bar{U}_h^2}, \quad C_{\hat{p}} = \frac{\hat{p}}{\frac{1}{2}\rho\bar{U}_h^2},$$
$$C_{\check{p}} = \frac{\check{p}}{\frac{1}{2}\rho\bar{U}_h^2}$$

Where, ρ is the density of air and \bar{U}_h is the mean velocity at roof height. The mean and peak pressure distributions were used to identify regions experiencing large wind loads, and for comparisons with data given in AS/NZ 1170.2. This AS/NZS 1170.2 equivalent quasi-steady aerodynamic shape factor $C_{fig} = C_{peak}/G_u^2$, where $G_u = (\hat{U}_h/\bar{U}_h)$ is the velocity gust factor. Here \hat{U}_h and \bar{U}_h are the 0.2 s gust wind speed and mean wind speed respectively at roof height.

Pressure distributions

The average of the minimum pressure coefficients obtained for approach winds within a 45° sector was used to derive the pressure distributions used for eight cardinal directions. The wind pressure distributions for a cornering wind sector 225

±20° is shown in

Figure 5. These wind tunnel derived pressures account for local pressure effects in flow separation regions and are used for the application of load to cladding and immediate supporting members such as batten to rafter connections. The pressures are factored by 0.5 for load application to major structural elements to account for area averaging effects of pressure fluctuations on the tributary area of the element.

Analysis of pressure coefficients with wind direction θ , show that the windward edge of the roof experiences the largest (mean and peak) suction pressures and the (windward) wall is subjected to positive pressures. These pressures are generally close to values given in AS/NZS1170.2. The underside of the eaves are subjected to pressures similar to that on the adjacent wall surface. Roof cladding, battens and rafters near the windward gable-end experience the largest wind pressures.

Internal pressure coefficients are calculated following the logic contained in the wind loading standard AS/NZS 1170.2 depending on the distribution and sizes of openings in the walls. The presence of openings is determined by modelling debris impact during a storm and pressure-induced failures of windows and doors.

The internal pressure in the nominally sealed house with the envelope intact is small, i.e. the internal pressure coefficient $C_{pi} = 0$. However, the failure of a door or window on the windward wall from wind pressure or debris impact with increasing wind speed can result in the internal pressure reaching the values of the external wall pressure at the dominant opening $C_{pi} = 0.6$ or more.

Connection strengths

Connection strengths are derived from engineering judgement and testing conducted at the Cyclone Testing Station. Some strengths are modified to account for load sharing effects. Strengths are assigned to connections in the VAWS model using log-normal probability distribution functions, with the mean strengths and coefficients of variation shown in Table 1.

Damage costing data

Cost of damage is calculated based on the number of failed connections, with each connection type corresponding to a tributary area in m² that would be affected during a failure, as shown in Table 2. Cost of damage in dollars is then calculated based on the envelope repair rate shown in Table 2. A damage index is calculated based on the ratio of the repair cost to the cost for full replacement of the house. In this case study, the replacement cost is set to the replacement cost for the roof and associated linings and finishes such as ceilings, eave linings, cornices and painting. This ensures that damage indices will reach 1.0 for complete failure. Costs associated with wall debris damage, loss of wall cladding, wall collapse and racking are not modelled in this case study.

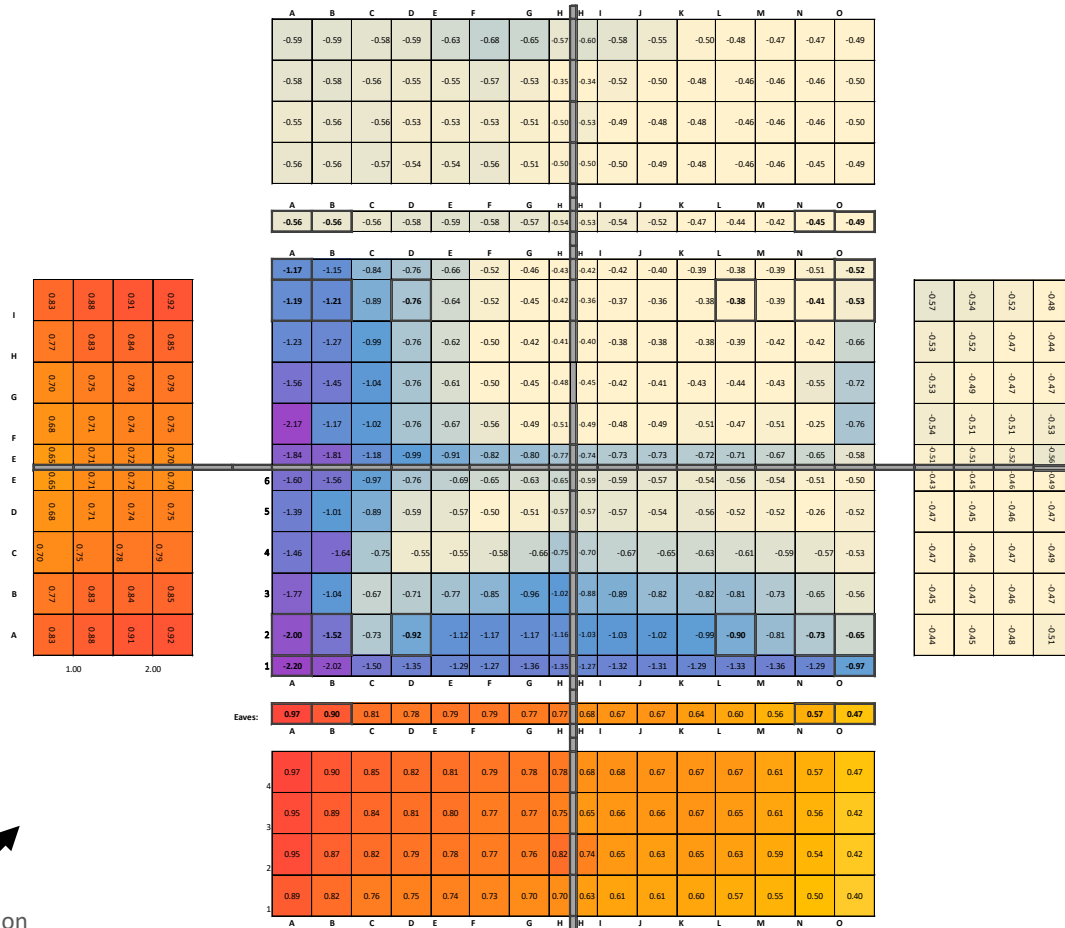


Figure 5: C_{ftg} pressure distribution for the sector $225 \pm 20^\circ$ on the roof, walls and the underside of the eaves of the wind tunnel model.

Table 1: Connection strengths.

Connection Type	Strength mean (kN)	CoV
Sheeting (for approx. 4 fasteners)	2.7	0.1
Batten to Rafter Connection	1.5	0.3
Rafter to Top Plate Connection	5	0.3

Table 2: Damage costing coverages and unit costs.

Failure Mode	Total Surface area [m^2]	Envelope repair rate [$\$/m^2$]
Loss of roof sheeting	113.4	72.40
Loss of roof sheeting & battens	113.4	184.2
Loss of roof structure	113.4	317.0

Results

Results for a single realisation

As described in previous sections, the VAWS software simulates the failure of connections and redistribution of loads to neighbouring connections in detail. Although several simplifying assumptions are involved, the vulnerability curves determined are based on structural failure behaviour that would occur during a wind storm.

Results for a single realisation of the wind and structure simulation for a south west wind direction are presented in this section. The external pressure distribution on the roof of the house is shown previously in Figure 5. The connection strengths within the house for this

realisation that were sampled from the log-normal probability distributions shown in Table 1 are shown in Figure 6.

The VAWS program does not run a time history of wind pressures but increases the wind speed in increments to represent the increase in wind speed through a wind storm. Based on the repair cost and cost for full replacement, a damage index is calculated for each wind speed increment. As damage increases with increasing wind speed, the data points of damage index trace a vulnerability function for that house realisation, shown in

Figure 7 . The onset of damage occurs at approximately 37 m/s with complete damage to the roof structure for this realisation (damage index =1) occurring at approximately 45 m/s, due the failure of rafter to top plate connections with increased loads due to internal pressurisation from debris impact.

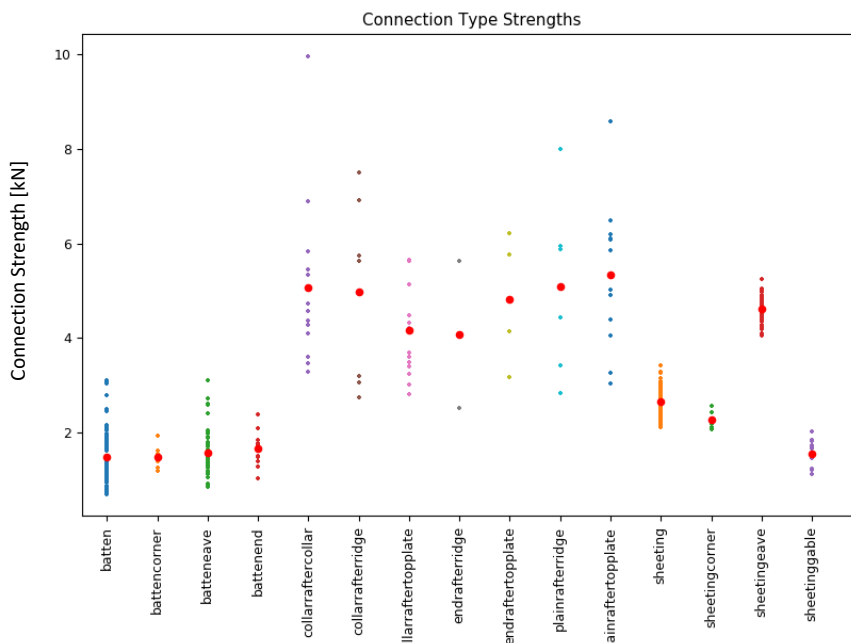


Figure 6: Sampled connection strengths for a single realisation of the Group 4 House, red dots indicate the mean.

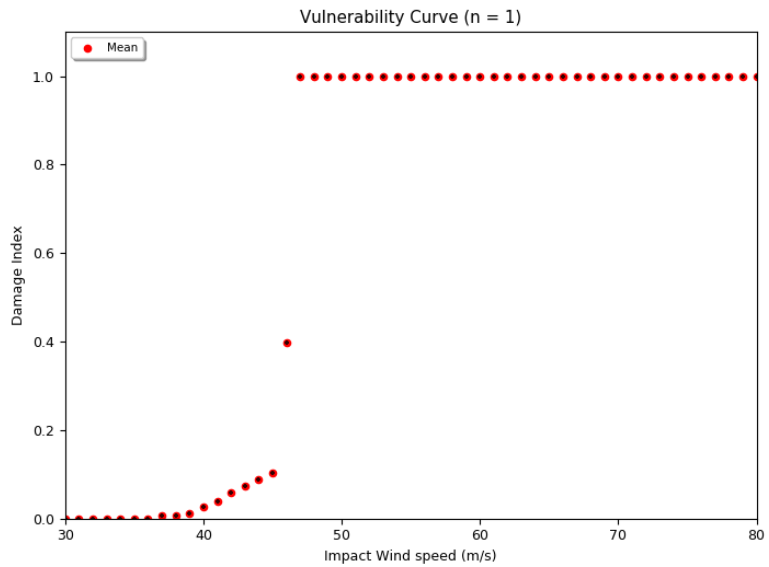


Figure 7: Vulnerability curve for a single realisation of the Group 4 House.

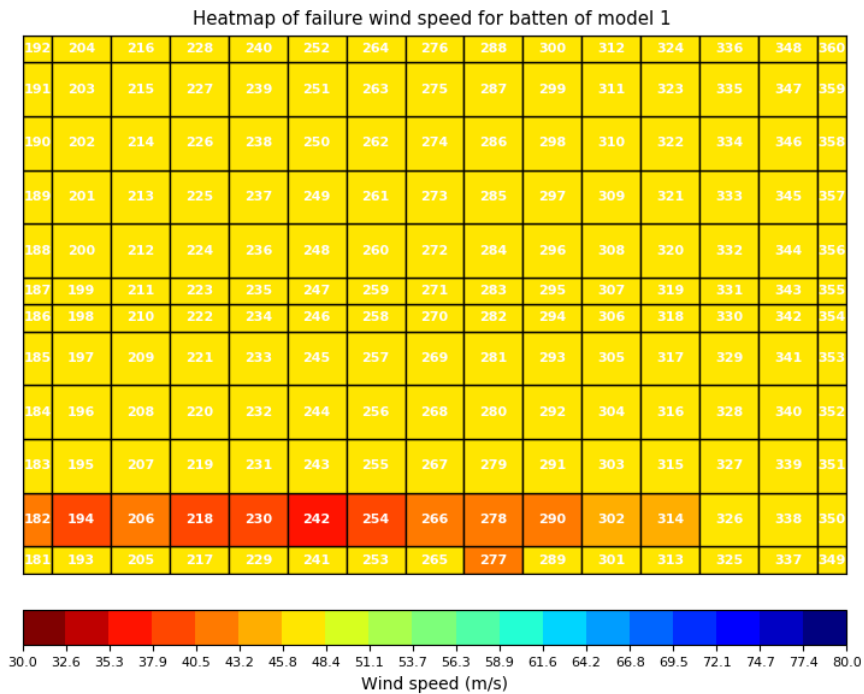


Figure 8: Plan view of house roof showing failure wind speeds for batten to rafter connections for a single model run at wind direction $225 \pm 20^\circ$. Note that large swathe of yellow indicating failure of all remaining connections at about 45 m/s caused by internal pressurisation.

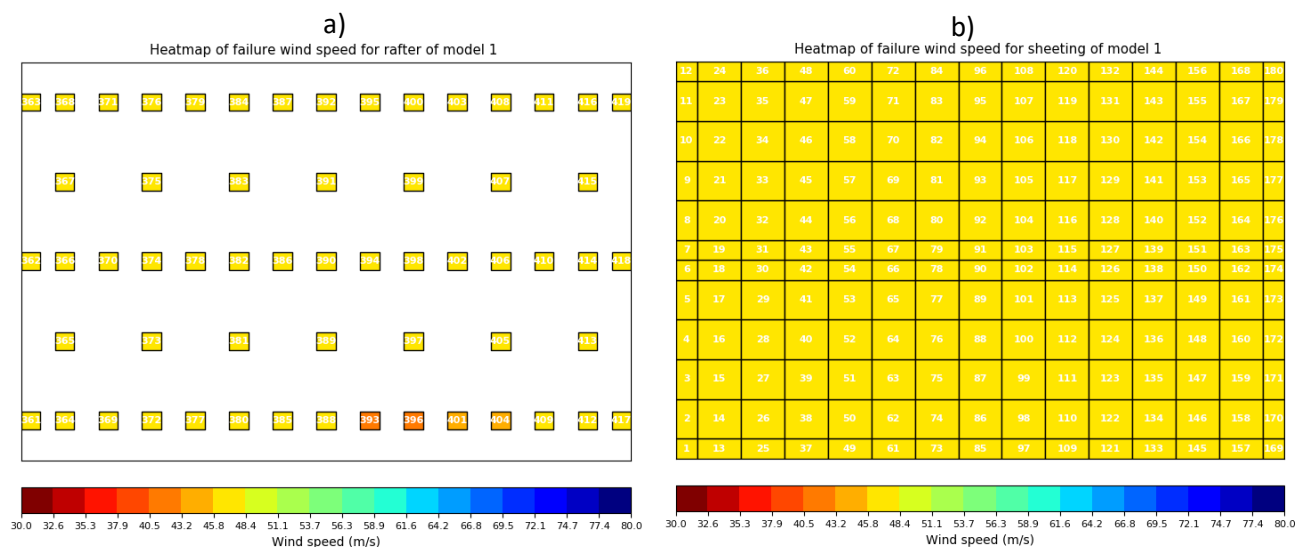


Figure 9: Plan view of house roof showing failure wind speeds for roof to wall connections and collar ties (a) and roof cladding (b) for a single model run at wind direction $225 \pm 20^\circ$. Note the numerous connections coloured yellow denoting failure at about 45 m/s caused by internal pressurisation.

Damage to the structure is presented in a series of 'heat maps' that show the gust wind speeds at failure of three different types of connections. These diagrams indicate how loads are redistributed and how damage spreads through the structure. Locations of initiation and spread of failure through the structure is indicated by bands or sections of roof zones that fail at a range of increasing wind speeds.

For this realisation, the batten to rafter connections are the first to fail at a wind speed of approximately 37 m/s, as shown in

Figure 8. This is expected for this house type, where batten to rafter connections are generally the weakest link in the tie down chain. Batten to rafter failures cause loads to be redistributed to neighbouring intact batten to rafter connections along the same batten to the left and right. For a SW wind direction, failure initiates at the second batten in from the windward roof edge (connection no. 242). Failure then propagates along the batten towards the left and right with increasing wind speed increments.

Load redistribution due to roof to wall connection failures is determined by varying influence coefficients for vertical reaction forces of failed connections and adjacent connections. For this realisation, roof to wall connection failure initiates near the middle of the roof (Figure 9a) and is due to high loads being transferred here due to the failure of batten to rafter connections (Figure 8) initiated to the left of this location.

For this realisation, internal pressurisation occurs due to debris impact on a door or window at about 45 m/s, as shown in

Figure 10. The sudden increase in loads immediately causes the failure of remaining roof to wall connections. Roof cladding failure causes loads to be redistributed to other cladding fasteners on neighbouring battens i.e. loads are redistributed along the direction parallel to the roof

corrugations. However, in this realisation the cladding fasteners sustain no damage, but all fasteners are costed as failures when the entire roof structure is removed due to internal pressurisation as shown in Figure 9 b).

Results for multiple realizations

The main purpose of VAWS is to determine vulnerability functions for a population of similar types of houses. Using a desktop computer, the VAWS program can run hundreds of realizations of a house type within minutes to determine vulnerability functions for a population of houses. The results of 100 realizations of the Group 4 House type are presented in this section. Each realization is assigned a wind direction, gust wind speed profile, external pressure coefficients and connection properties. Load redistribution and connection failures are calculated for each realization as described in the previous section and internal pressurization is determined based on the debris impact module.

The damage index based on cost of repair for each realization is calculated at increasing wind speed increments and the results for each realization (black dots) together with mean damage index (red dots) are shown in Figure 11. The wind speeds causing the onset of damage for most of the houses ranges from 35 to 45 m/s and complete damage occurs from 45 to 55 m/s. Such onset and complete damage thresholds are similar to observations from post windstorm damage investigations conducted by the Cyclone Testing Station (Boughton et al., 2017).

In this case study, two realizations do not experience complete structural damage even at very high wind speeds (80 m/s). These particular realizations are those where the failure of a leeward window has caused a negative pressure within the building, thus reducing uplift loads on the roof structure. Such reductions in pressure are possible in reality, however, wall racking failures that are not modelled in this case study would most likely occur at such high wind speeds. As such, the non-failure behavior of the two realizations is largely artificial.

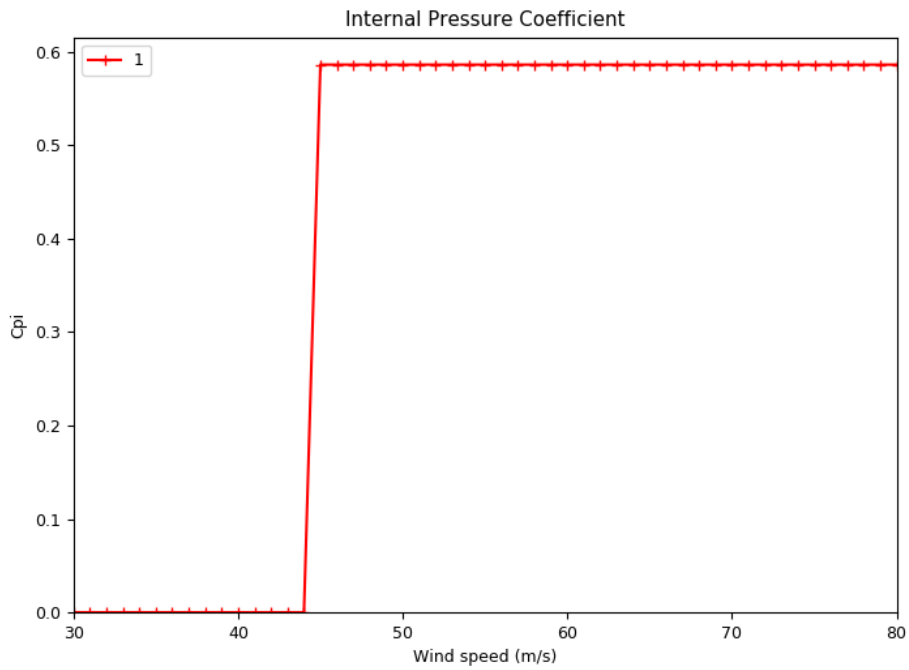


Figure 10: Internal pressure coefficients for a single realisation (red line) as a function of wind speed, indicating internal pressurisation occurring at approx. 45m/s due to debris impact.

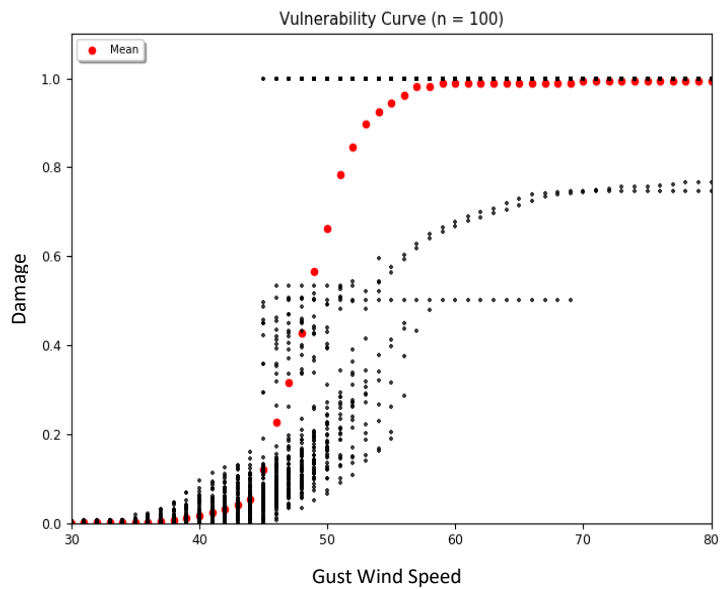


Figure 11: Vulnerability results for 100 realisations of the Group 4 House. The horizontal axis is the 0.2 s gust wind speed at 10m at the house of interest.

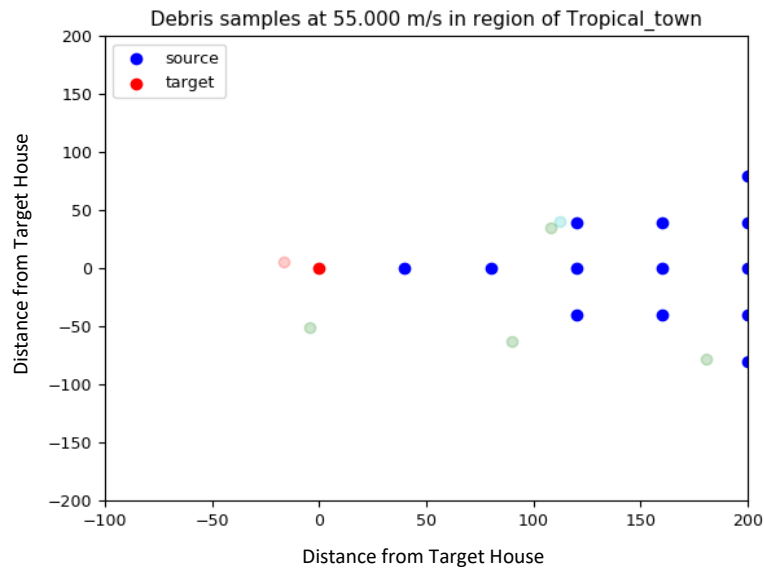


Figure 12: Debris sources and the target house. Faint cyan, green and red dots represent the landing sites of compact, sheet and rod shaped debris items respectively.

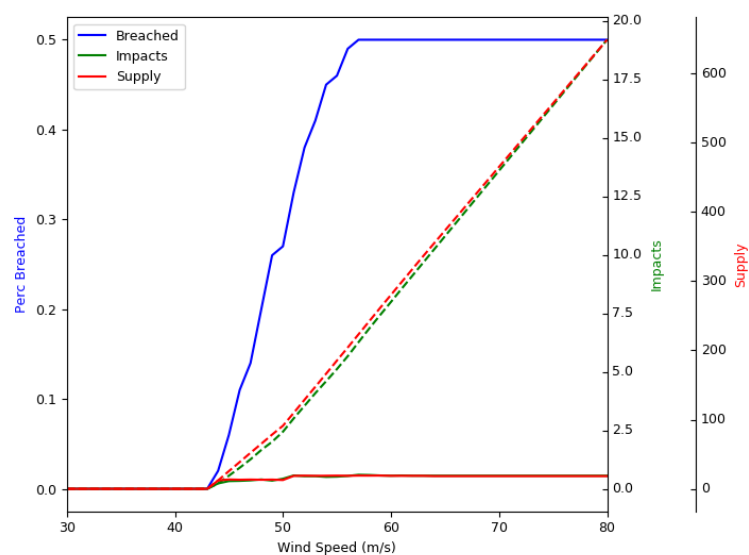


Figure 13: Debris generation, impacts and percentage of envelop breaches as a function of wind speed. Debris item supply and impacts are shown as red and green lines respectively. The plots of debris item supply and impacts are provided for individual wind speeds (solid lines) and also as a cumulative plot (dashed lines).

Windborne Debris and Internal Pressures:

The trajectories, generation and exhaustion of windborne debris is modelled in detail through a process described in Wehner et al. (2010b). An example of debris landing locations, sources and the target house, for a single realization at a single wind speed are shown in Figure 12.

The modelling of debris allows for cost of damaged wall cladding to be determined, more importantly breaches of the building envelope through broken windows trigger the internal pressurization of the house. The overall percentage of breached houses in the population increases from zero to approximately 50% as wind speeds increase from 40 to 55 m/s, shown in Figure 13.

Calibration

The VAWS software output is checked based on engineering judgement and observations from past damage surveys. Additionally, the heuristic vulnerability curves (Timber Ed, 2006) provide a starting point for validating the output of VAWS. Furthermore, structural behavior is assessed using individual runs with a single wind direction and studying only one connection failure mode at a time. Results are compared with more detailed studies by Parackal (2018).

Conclusions

This paper outlined the overall logic of the VAWS software package and presented a case study of high-set Northern Australian house type. The VAWS program quantifies the vulnerability of a population of house types in Australia accounting for the variability in wind speed, external and internal pressures, debris impacts and connection strengths. Significant advances in modelling compared to previous empirical vulnerability models lie in the simulation of debris impacts and in the load redistribution and progressive failures of connections in the structure. The software allows the reduction in vulnerability afforded by retrofit to be easily modelled by re-running a simulation with the connection strength parameters adjusted to suit the strengthening work.

The case study presented demonstrated load redistribution and spread of failure in the Group 4 House for increasing wind speeds. Although several simplifying assumptions are used to model failure efficiently, the modelled behavior estimates a similar extents of failure that would occur in a windstorm.

The simulation of 100 realizations of the Group 4 House allowed the fitting of vulnerability curves to the calculated damage index at each wind speed increment. Wind speeds of onset and complete failure of houses compare satisfactorily with observations from damage investigations. Next steps in the development of VAWS include the modelling and calibration of wall racking failures, water ingress costs and assessing the vulnerability of several other Australian house types.

References

Boughton, G, Falck, D, Henderson, D, Smith, D, Parackal, K, Kloetzke, T, Mason, M, Krupar, R, Humphreys, M, Navaratnam, S, Bodhinayake, G, Ingham, S & Ginger, J 2017, *Tropical Cyclone Debbie: Damage to buildings in the Whitsunday Region*, Cyclone Testing Station, JCU, Report TR63.

Geoscience Australia 2019, *VAWS User Manual v.3.01*.

Henderson, D & Ginger, J 200, 'Vulnerability model of an Australian high-set house subjected to cyclonic wind loading, *Wind & Structures*, vol. 10, pp. 269-285.

Henderson, D & Harper, B 2003, *Climate change and tropical cyclone impact on coastal communities' vulnerability*, Queensland Government (Dept. of Natural Resources and Mines, and Dept. of Emergency Services), Brisbane, Australia.

Holmes, J & Best, R 1978, 'Wind Pressures on an Isolated High-Set House', *Wind Engineering Report 1/78*, James Cook University of North Queensland.

Parackal, K 2018, *The Structural Response and Progressive Failure of Batten to Rafter Connections under Wind Loads*, PhD Thesis, James Cook University.

Standards Australia 2011, *Structural design actions Part 2: Wind actions*, AS/NZS1170.2, Sydney, Australia.

Timber ED 2006, *Report on Wind Vulnerability Research Workshop*, Geoscience Australia, James Cook University.

Wehner, M, Ginger, J, Holmes, J, Sandland, C & Edwards, M 2010a, 'Development of methods for assessing the vulnerability of Australian residential building stock to severe wind', *IOP Conference Series: Earth and Environmental Science*, vol. 11, 012017.

Wehner, M, Sandland, C, Holmes, J, Henderson, D & Edwards, M 2010b, 'Modelling damage to residential buildings from wind-borne debris - Part 1, methodology', presented at the *14th Australasian Wind Engineering Society Workshop*, Canberra, Australia, pp. 58-61.